The Effect of Composition and the Introduction of Positive Charge Group (—$N(CH_3)_2$) on the Multiphase Morphology of Polyurethane/Polyacrylates Interpenetrating Polymer Networks

XIAOQIANG YU, JINGYUAN WANG, GE GAO, JUN TANG, FENG LI, JIDONG ZHANG, XINYI TANG

Department of Chemistry, Jilin University, 130023 Changchun, China

Received 12 November 1998; accepted 14 January 1999

ABSTRACT: A series of interpenetrating polymer networks (IPNs) of polyurethane/polyacrylates were synthesized. Their morphology was investigated by means of small-angle X-ray scattering (SAXS) and transmission electron microscope (TEM). The influence of an active positive charge group (—$N(CH_3)_2$) on the phase structure of the aforementioned IPNs was studied. The results show not only that the size of phase segregation zones varies with composition but also that the specific interfacial surface areas have a maximum when the weight ratio of polyurethane and polyacrylates is 1 : 2. Moreover, the introduction of an active positive charge group (—$N(CH_3)_2$) is an important way of increasing the miscibility between two component polymers. © 1999 John Wiley & Sons, Inc. J Appl Polym Sci 74: 1898–1904, 1999

Key words: IPNs; morphology; SAXS; miscibility

INTRODUCTION

Interpenetrating polymer networks (IPNs) are defined as a combination of two or more polymers in a network form, in which at least one of them is synthesized and/or crosslinked in the immediate presence of the other.[1,2] When both polymers are polymerized and crosslinked simultaneously with noninterfering modes, such as stepwise and chain polymerization, the IPN is known as a simultaneous interpenetrating network (SIN).[3,4]

A number of studies have shown that the domain size, shape, two-phase cocontinuity, and phase separation have important effects on the physical, chemical, thermal, and mechanical properties of IPN materials.[5–7] Thus, the determination of the morphological structure has become a very important research topic in the field of IPN technology.[7–10] Recently, TEM, dynamic mechanical spectroscopy, SAXS, and small-angle neutron scattering (SANS) have been used extensively to characterize the morphological structure.[11–14] Several authors have used SAXS and SANS techniques to obtain diverse information about polymer structure. Early in the 1980s, An and colleagues[15] investigated the domain formation processes in poly(*cross*-butadiene)-*inter*-poly(*cross*-styrene) IPNs by SANS and TEM. Their experimental data supported the interconnected cylinder model of IPNs. Later, Tan and coworkers[16] used the Debye and Guinier methods to determine the short-range correlation length and the correlation length of poly(polyethylene glycol diacrylate)/epoxy resin IPNs. They showed that the size of the phase segregation zones changed with composition. Most recently, Junker and coworkers[17] demonstrated the composition and temperature dependence of SIN by observing the

Correspondence to: J. Wang.

Journal of Applied Polymer Science, Vol. 74, 1898–1904 (1999)
 CCC 0021-8995/99/081898-07

Table I Materials Used in the Preparation of the IPNs

Material Description	Source	Code
Tolylene diisocyanate (TDI)	Shanghai Chemical Co.	TDI
Hydroxylgroup-terminated butadiene–acrylonitrile copolymer (PBAO)	Changchun Institute of Applied Chemistry	PBAO
Trimethylol propane (TMP)	Beijing Chemical Co.	TMP
Methyl methacrylate (MMA)	Jiangsu Chemical Co.	MMA
Ethyl methacrylate (EMA)	Jiangsu Chemical Co.	EMA
Butyl methacrylate (BMA)	Jiangsu Chemical Co.	BMA
N,N-Dimethylethanolaminic ethacrylate (DMA)	Chenguang Chemical Co.	DMA
Trimethylolpropanoic trimethacrylate (TMPTMA)	Beijing Chemical Co.	TMPTMA
Benzoyl peroxide (BPO; MMA, etc. initiator)	Shenyong Chemical Co.	BPO
Dibutyltin dilaurate (PU catalyst)	Shanghai Chemical Co.	T12

results of SAXS experiments. Their conclusions were that the maximum in scattering intensity cannot be described by the Debye–Bueche theory,[25] whereas it is in agreement with the hydrodynamic structure factor. However, as yet, these studies are much less extensive.

The polyurethane/polyacrylates interpenetrating polymer networks have a potential practical value for noise and vibration damping.[8,18–24] Thus, it is of fundamental and technological significance to determine the microstructure of these IPN materials. Also of paramount importance is a clear understanding of the mechanisms of the morphological change. In this article, a series of polyurethane/polyacrylates interpenetrating polymer networks have been synthesized. The parameters about morphological structure of these IPNs, such as the correlation distance and the specific surface area, were determined by SAXS and TEM. The effect of the composition and the introduction of positive charge group (—$N(CH_3)_2$) on the morphological structure is discussed.

EXPERIMENTAL

Materials

The raw materials are listed in Table I. They were used without further purification.

Synthesis

The hydroxylgroup-terminated butadiene–acrylonitrile copolymer ($\bar{M}_n$ = 2500 g/mol; acrylonitrile, 5 wt %) was dissolved in the mixed solvent of 2-butanone and ethyl acetate. Then methyl methacrylate (MMA), ethyl methacrylate (EMA), *N,N*-dimethylethanolaminic ethacrylate (DMA), or *n*-butyl methacrylate (*n*-BMA), trimethylolpropanoic trimethacrylate (TMPTMA), and benzoyl peroxide (BPO) were added to the aforementioned solution with vigorous stirring at room temperature. The mixture was heated to approximately 80 to 90°C and kept at this temperature for about 1 h to give a yellow and viscous solution. Bubbles were produced in the mixture with the addition of tolylene diisocyanate (TDI), trimethylol propane (TMP), and T12. After standing at 80°C for 10 min, the mixture was cooled to room temperature. At this time, the mixture was poured as a film with a thickness of approximately 2 to 3 mm and was dried at atmosphere for 2 h. Finally, it was cured at 80°C for approximately 2 to 3 h. The NCO/OH ratio was 1.05 for all IPN samples. To investigate the effect of the composition, samples 1 to 5 were prepared, in which the molar quantities of the positive charge group (—$N(CH_3)_2$) in polyacrylates from DMA were equivalent to the molar quantities of the negative charge group (—CN) in polyurethane from hydroxylgroup-terminated butadiene–acrylonitrile copolymer. Moreover, samples 6, 7, and 8 were prepared to study the effect of the interaction of positive charge group (—$N(CH_3)_2$) and negative charge group (—CN) on the morphology of IPNs. In sample 8, the molar quantities of (—$N(CH_3)_2$) are half of the molar quantities of (—CN). All reactants and auxiliary compounds are listed in Table II.

SAXS Experimental

The small-angle X-ray scattering (SAXS) intensity of the samples was registered with a Kratky

Table II Recipes for the Preparation of the IPNs

Reagent (wt %)	Sample 1 (n-3/1)[a,b]	Sample 2 (n-2/1)[b]	Sample 3 (n-1/1)[b]	Sample 4 (n-1/2)[b]	Sample 5 (n-1/3)[b]	Sample 6 (1/2)[b]	Sample 7 (1/1)[b]	Sample 8 (n-1/2)[b]
TDI	5.60	5.02	3.74	2.47	1.87	2.47	3.74	2.47
PBAO	69.15	61.78	46.11	30.43	23.05	30.43	46.11	30.43
TMP	1.49	1.34	1.00	0.66	0.50	0.66	1.00	0.66
T12	0.15	0.13	0.10	0.07	0.05	0.07	0.10	0.07
MMA	6.94	11.52	21.24	31.04	35.7	8.71	21.24	32.27
EMA	6.94	11.52	21.24	31.04	35.7	28.71	21.24	32.27
DMA	11.12	9.97	7.52	4.91	3.59	—	—	2.46
BMA	—	—	—	—	—	9.57	7.52	—
TMPTMA	0.05	0.06	0.10	0.14	0.15	0.14	0.10	0.14
BPO	0.25	0.33	0.50	0.67	0.75	0.67	0.50	0.67

[a] n = contains DMA in IPNs.
[b] Represents the weight ratio of polyurethane (PU)/polyacrylate (PA).

compact camera (Anontpaar Company, Austria), in front of which was mounted directly on the top the cube shield of a stabilized Philips (Philips, the Netherlands) PW1170 X-ray generator. The Kratky X-ray tube was operated at a power of 1.5 kW. CuKα radiation was used; the monochromatization was performed by a Ni filter in conjunction with a pulse–height discriminator. Measurements were made by a step-scanning procedure in the fixed-time mode, with a sampling time of 200 s for each step. The number of steps was generally of the order of 250 for each sample. The entrance and detector slits were adjusted, respectively, to 80 and 200 μm. However, to approach the origin of the angles as closely as possible, the beginning of the curve was also registered with the entrance and detector slits adjusted to 42.5 and 107.5 μm, respectively, and this was then merged with the main part of the curve. The explored domain was thus $0.006 \leq s \leq 1$ nm^{-1}, where $s = 2 \sin \theta/\lambda$, with 2θ = scattering angle and λ = X-ray wavelength (0.1542 nm).

TEM Experimental

A small piece of each of the IPN samples was stained in 2% aqueous osmium tetroxide vapor for one week. The samples were trimmed and then thin-sectioned (500 nm), using a Reichert–Jung (Sweden) UltraCut E ultramicrotome. The electron micrograghs were observed in an H-500 transmission electron microscope (Hitachi, Japan). The polyurethane phase is stained with the osmium tetroxide and appears as the darker area in TEM micrographs.

RESULTS AND DISCUSSION

Theoretical Background[25–29]

The SAXS scattering theory can be summarized as follows: For a two-phase system where one phase is dispersed in the other phase, the scattering intensity satisfies the Debye–Bueche equation

$$I_{(S)} = K_2 \langle \eta^2 \rangle_{av} \int_0^\infty \gamma_a(\gamma)[\sin(2\pi sr)/2\pi sr] r^2 \, dr \quad (1)$$

where K_2 is a constant; η is the power fluctuation of the scattering system, which equals the difference between the electron density at the scattering angle and the average value; $\gamma_{a(}\gamma)$ is a correlation function; s (= 2 sin θ/λ) is a scattering vector in reciprocal space; 2θ is scattering angle; λ is the wavelength of the X ray that equals 0.1542 nm.

The correlation function can be obtained by the Fourier transformation of the scattering intensity. For the simplest case, the correlation function can be given by an exponential form as proposed by Debye and coworkers[26]:

$$\gamma_a(\gamma) = \exp(-\gamma/a_c) \quad (2)$$

The coefficient a_c represents the correlation distance that defines the size of heterogeneous phases. It follows that

$$I_{(S)} = K_2 \langle \eta^2 \rangle_{av} a_c^3 (1 + 4\pi^2 s^2 a_c^2)^{-2} \quad (3)$$

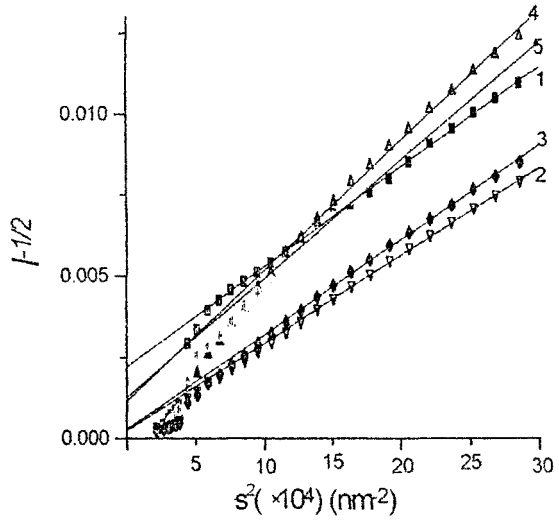

Figure 1 Debye plots of $I^{-1/2}$ versus S^2 for samples 1, 2, 3, 4, and 5. All plots show two straight zones.

Therefore, plotting $I_{(s)}^{-1/2}$ versus s^2, the so-called Debye plot, should produce a straight line from which the correlation length a_c can be given:

$$a_c = (\text{slope/intercept})^{1/2}/2\pi \tag{4}$$

The specific interfacial surface area S_{sp}, defined as the ratio of interfacial surface area S to the volume V is given by

$$S_{sp} = S/V = 4\varphi_p(1 - \varphi_p)/a_c \tag{5}$$

where φ_p represents the volume fraction of the first phase. In the present article, it was convenient to convert S_{sp} to m^2/g, using the known density of the system.

In addition, according to the Guinier equation

$$\ln I_{(s)} = \ln I_{(0)} - (4/3)\pi^2 s^2 R^2 \tag{6}$$

Plotting $\ln I_{(s)}$ versus s^2, the so-called Guinier plot, should produce a straight line with slope of $(4\pi^2R^2/3)$, and the radius of gyration can be given by

$$R = (3 \times \text{slope})^{1/2}/2\pi \tag{7}$$

The relation between the radius of gyration and the correlation parameters of morphology can be described as proposed by Liegeois and coworkers[29]:

$$a_c = 2R(\pi/3)^{1/2} \tag{8}$$

The transverse lengths across the domain, the average dimension obtained from straight lines drawn through the whole sample, are given by

$$l_1 = a_1/\varphi_2 \quad l_2 = a_1/\varphi_1 \tag{9}$$

where a_1 represents the correlation length determined by the Debye method.

The Effect of Composition on the Multiphase Morphology of IPNs

Figure 1 is a typical Debye plot displayed in terms of $I^{1/2}$ versus S^2. Two straight portions are observed. A straight line was drawn through the wide-angle portion, and the short-range correlation distance a_1 was determined from eq. (4). The excess intensity between the line determining a_1 and the lower-angle slope was determined by obtaining the difference between the line used to calculate a_1 and the line characterizing the lower-angle slope. Figure 2 is a typical Guinier plot in terms of ln I versus S^2. The intensity I was obtained from the preceding difference. The correlation distance a_2 and the radius of gyration R were determined in terms of eqs. (7) and (8). The several phase dimensions determined from a_1 and a_2 are listed in Table III.

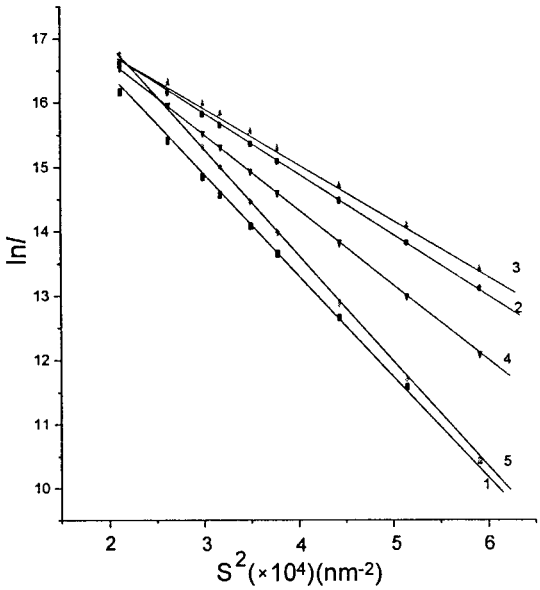

Figure 2 Guinier plots of ln I versus S^2 for samples 1, 2, 3, 4, and 5.

Table III Phase Dimensions of Polyurethane/Polyacrylate IPNs

Sample	PA Content (vol %)	Correlation Distance, A		Specific Interfacial Area, S_{sp} (m^2/g)	Transverse Length, A	
		a_1	a_2		l_A	l_U
1	25	132.0	339.8	594.9	176	528
2	33	170.2	265.6	541.2	254	516
3	50	163.5	259.0	630.5	327	327
4	67	129.7	299.0	695.3	393	193
5	75	115.5	356.6	659.2	462	154

According to the SAXS principle, the quantity a_1 measures the *intra*particle distance and the quantity a_2 measures the *inter*particle distance. Figure 3 is the electron micrograph of sample 4. The a_1 and a_2 vary with composition, as observed in Table III. Moreover, the size of cylinder calculated from the Debye plot is consistent with that observed from the electron micrograph.

As seen in Table III, a_2 is much larger than a_1 for each sample. Thus, one can take into consideration that quantity a_1 and quantity a_2 might represent the fine structure and the larger domain, respectively. The calculated transverse length of the polyacrylate domain l_A increases with the weight fraction of polyacrylate slowly. The most interesting quantity is S_{sp}, which presents a maximum when the weight ratio of polyurethane and polyacrylate is 1 : 2. An acceptable interpretation is that the phase domain structure in IPNs produces reorganization at this weight ratio. For this IPN system, this would mean that extensive interpenetration between two components occurs. It should be pointed out that S_{sp} is dependent of morphological model. It assumes a random phase arrangement.

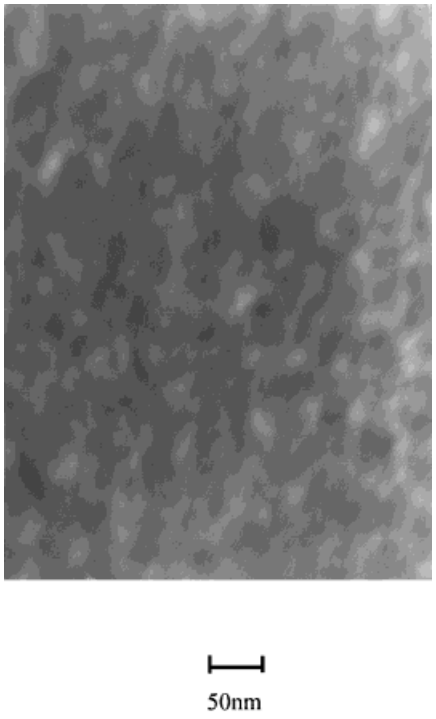

Figure 3 Transmission electron micrographs of sample 4.

The Effect of the Introduction of Positive Charge Group (—$N(CH_3)_2$) on the Multiphase Morphology of IPNs

Figure 4 and Figure 5 are, respectively, the Debye plots and Guinier plots of samples 6, 8, 4, 7, and 3.

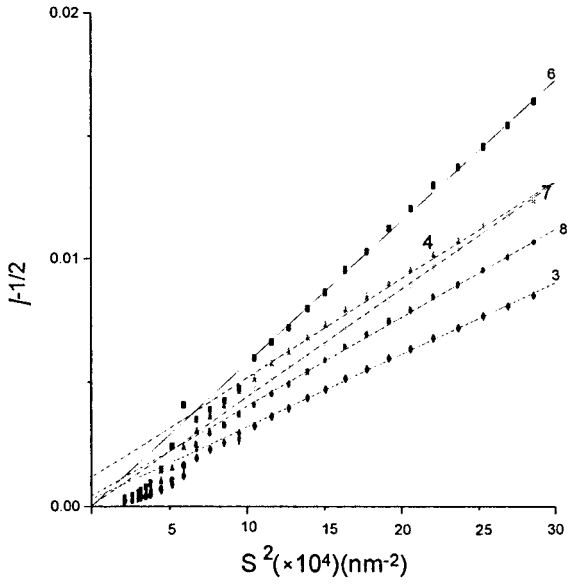

Figure 4 Debye plots of $I^{-1/2}$ versus S^2 for samples 6, 8, 4, 7, and 3. All plots show two straight zones.

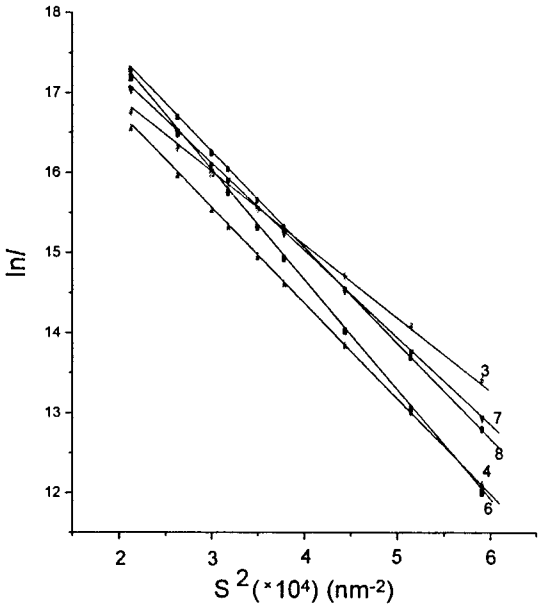

Figure 5 Guinier plots of ln I versus S^2 for samples 6, 8, 4, 7, and 3.

From Figures 4 and 5, the short-range correlation distance a_1 and the correlation distance a_2 can be calculated. Several phase dimensions determined from a_1 and a_2 are listed in Table IV.

As seen in Table IV, when the positive charge group (—$N(CH_3)_2$) was introduced into the IPNs, the short-range correlation distance a_1, the transverse length of polyacrylate phase l_A, and the transverse length of polyurethane l_U decrease due to the interattraction between the (—$N(CH_3)_2$) and the negative charge group (—CN). This means that the miscibility between two components increases. Figure 6 is the electron micrograph of sample 6. The results from TEM (see Fig. 6 and Fig. 3) support the conclusions obtained from SAXS. The specific interfacial surface area

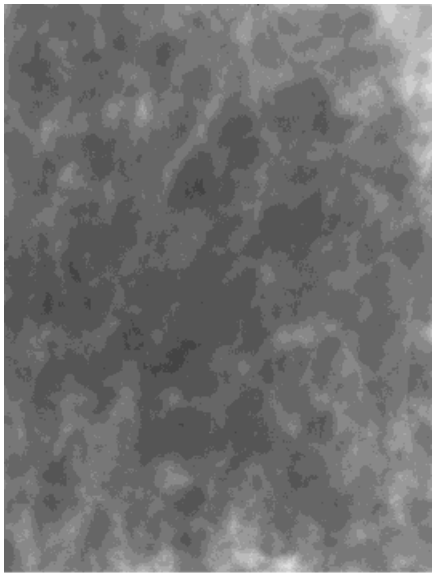

Figure 6 Transmission electron micrographs of sample 6.

S_{sp} increases with the content of positive charge group (—$N(CH_3)_2$), which shows that the more extensive interpenetration between two components occurs due to the strong interattraction between opposite charge groups.

CONCLUSIONS

This study indicates that the SAXS technique can provide much valuable information about

Table IV Phase Dimensions of Polyurethane/Polyacrylate IPNs

Sample	PA Content (vol %)	Correlation Distance, A		Specific Interfacial Area, S_{sp} (m^2/g)	Transverse Length, A	
		a_1	a_2		l_A	l_U
6	67 (0 : 1)[a]	150.0	322.4	601.6	454	223
8	67 (1 : 2)	147.2	299.9	613.0	445	219
4	67 (1 : 1)	129.7	298.0	695.7	393	193
7	50 (0 : 1)	182.2	287.8	565.8	364	364
3	50 (1 : 1)	163.5	259.0	630.5	327	327

[a] The expression in parentheses represents the molar ratio of (—$N(CH_3)_2$) and (—CN).

IPN morphology, such as the short-range correlation distance, the transverse length of domain, the interfacial area, and so forth. Combining with other methods, such as TEM, the SAXS provides a powerful new method of analysis for investigating the miscibility and the degree of interpenetration of two-component networks in an IPN system.

The morphology and the interfacial surface area S_{sp} of the polyurethane/polyacrylates interpenetrating polymer networks vary with composition. The interattraction between the positive charge group in the dispersed phase (polyacrylate) and the negative charge group in the continuous phase (polyurethane) will improve the miscibility between two components.

REFERENCES

1. Sperling, L. H. Interpenetrating polymer networks and related materials; Plenum: New York, 1981.
2. Klempner, D.; Frisch, K. C. Advances in interpenetrating polymer networks, Vol.2; Technomic Publishing Co.: Lancaster, PA, 1990.
3. Lee, D. S.; Park, S. J Appl Polym Sci 1991, 43, 481.
4. Chiang, W. Y.; Chang, D. M. Eur Polym J 1995, 31, 709.
5. Charkabarty, D.; Das, B. J Appl Polym Sci 1996, 60, 2125.
6. Jang, B. Z.; Pater, R. H.; Sovcer, M. D. J Polym Sci Part B: Polym Phys 1992, 30, 643.
7. Dadbin, S.; Burford, R. P.; Chaplin, R. P. Polymer 1996, 37, 785.
8. Wang, J.; Liu, R.; Li, W.; Li, Y.; Tang, X. Polym Int 1996, 39, 101.
9. Lipatov, Y. S. Macromol Chem Phys (C) 1990, 30, 209.
10. Frounchi, M.; Burford, R. P.; Chaplin, R. P. Polymer 1994, 35, 5073.
11. Brovko, O. O.; Sergeeva, L. M.; Slinchenko, O. A. Polym Int 1996, 40, 299.
12. Hourston, D. J.; Schafer, F. U.; Bates, J. S. J Appl Polym Sci 1996, 59, 203.
13. Nagarajan, P.; Trivedi, M. K.; Mital, C. K. J Appl Polym Sci 1996, 59, 203.
14. Schulze, U.; Fiedwerova, A.; Pompe, G.; Meyer, E. Polymer 1998, 39, 1289.
15. An, J. H.; Fernandez, A. M.; Sperling, L. H. Macromolecules 1987, 20, 191.
16. Tan, S. S.; Zhang, D. H.; Zhou, E. L. Polym Int 1997, 42, 90.
17. Junker, M.; Alig, I.; Frisch, H. L.; Fleischer, G.; Schulz, M. Macromolecules 1997, 30, 2085.
18. Foster, J. N.; Sperling, L. H. J Appl Polym Sci 1987, 33, 2637.
19. Klempner, D.; Sophiea, D.; Suthar, B.; Frisch, K. C. Polym Mater Sci Eng 1991, 65, 82.
20. Tung, C. J.; Hsu, T. J. J Appl Polym Sci 1992, 46, 1759.
21. Li, Y.; Liu, R.; Wang, J.; Tang, X. Prog Org Coating 1992, 21, 101.
22. Usman, A. S.; William, L. Y.; Timothy, L. D. U.S. Pat. 5,225,498, 1993.
23. Usman, A. S.; William, L. Y.; Timothy, L. D. U.S. Pat. 5,331,062, 1994.
24. Xie, H.; Wang, G.; Guo, J. Die Angewandte Makromolekulare Chemie 1994, 221, 91.
25. Debye, P.; Bueche, A. M. J Appl Phys 1949, 20, 518.
26. Debye, P.; Anderson, H. R., Jr.; Brumberger, H. J Appl Phys 1957, 28, 679.
27. Moritani, M.; Inone, T.; Motegi, M.; Kawai, H. Macromolecules 1970, 3, 433.
28. Alexander, L. E. X-Ray Diffraction Methods in Polymer Science; John Wiley: New York, 1969.
29. Sobry, R.; Rassel, Y.; Fontaine, F.; Ledent, J.; Liegeois, J. M. J Appl Crystallogr 1991, 24, 692.